Experimental and Theoretical Investigation of Valence Orbitals in 1,4-Dioxane by Electron momentum Spectroscopy

2006 Chinese Phys. Lett. 23 1157

(http://iopscience.iop.org/0256-307X/23/5/026)

Experimental and Theoretical Investigation of Valence Orbitals in 1,4-Dioxane by Electron momentum Spectroscopy *

YANG Tie-Cheng(杨铁成), NING Chuan-Gang(宁传刚), SU Guo-Lin(苏国林), DENG Jing-Kang(邓景康)**, ZHANG Shu-Feng(张书锋), REN Xue-Guang(任雪光), HUANG Yan-Ru(黄艳茹)

Department of Physics and Key Laboratory of Atomic and Molecular NanoSciences of MOE, Tsinghua University, Beijing 100084

(Received 11 January 2006)

*The binding energy spectrum of all valence orbitals and the momentum distributions of highest occupied molecular orbital (HOMO: $8a_g$), $7b_u+7a_g$, $4b_u$, $2b_g+4a_g$ and $2a_u$ in 1, 4-dioxane are investigated by electron momentum spectroscopy (EMS) with 600 eV impact energy. The experimental results are consistent with theoretical calculations of C_{2h} chair conformation using the Hartree–Fock method and density functional theory with 6-311++G** and AUG-CC-PVTZ basis sets.*

PACS: 33. 15. Ry, 34. 80. Gs, 36. 20. Kd

It is well known that 1,4-dioxane ($C_4H_8O_2$) is a six-member heterocyclic ring. It is an important solvent for polymers[1] and is also used as a stabilizer in chlorinated solvents, particularly 1,1,1-trichloroethane (TCA).[2] The molecular structure of 1,4-dioxane has been studied by several experimental methods such as x-ray and neutron diffraction,[1] infrared and NMR spectroscopy,[3−5] and theoretical calculations have been carried out by using ab initio theory at HF/6-31G* and BLYP/6-31G* levels.[6] According to the experimental and theoretical results, a chair form of C_{2h} symmetry has been determined to be the lowest energy structure.

Electron momentum spectroscopy (EMS), also known as binary $(e,2e)$ spectroscopy, can provide a direct imaging of electron density for molecular orbitals in momentum space, and has been shown to be a powerful and informative experimental tool for studying the electronic structure of atoms, molecules, biomolecules, and condensed matter.[7−9] In this Letter, the EMS study of 1,4-dioxane is reported, and the experimental results are compared with the theoretical calculations of C_{2h} chair form carried out by using Hartree–Fock (HF) method and density functional theory (DFT) with 6-311++G** and AUG-CC-PVTZ basis sets.

Electron momentum spectroscopy is based on binary $(e,2e)$ reaction. An incident electron with energy E_0 causes the ionization of the target molecule, by detecting the two outgoing (scattered and ionized) electrons in coincidence with energies E_1 and E_2, polar angles θ_1 and θ_2 and a relative azimuthal angle ϕ, the EMS kinematics of the target molecule can be completely determined. Under the binary encounter requirements of high impact energy and high momentum transfer and with the symmetric non-coplanar experimental geometry, in which the two outgoing electrons are selected to have equal energies ($E_1 \approx E_2$) with equal polar angles ($\theta_1 = \theta_2 = 45°$) and a varying relative azimuthal angle ϕ, the initial electron momentum p of the molecule is given by

$$p = \left[(2p_1\cos\theta - p_0)^2 + \left(2p_1\sin\theta\sin\left(\frac{\phi}{2}\right)\right)^2\right]^{1/2}, \quad (1)$$

where p_0 is the momentum of the incident electron and p_1 is the momentum of the outgoing electrons.

Within the plane wave impulse and the target HF approximations, the EMS cross section for randomly oriented gas-phase molecules can be given by[7]

$$\sigma_{\rm EMS} \propto \int d\Omega |\Psi_j(\boldsymbol{p})|^2, \quad (2)$$

where $\Psi_j(\boldsymbol{p})$ is the one-electron momentum space canonical HF orbital wavefunction for the jth electron, corresponding to the orbital from which the electron is ionized. The integration $\int d\Omega$ gives the spherical average over the random orientations of the target molecules. The integral in Eq. (2) is known as the spherically averaged one-electron momentum distribution. To this extent, EMS has the ability to image the electron density distribution in individual orbitals selected according to their binding energies.

In the DFT, the target Kohn–Sham approximation[10] gives a result similar to Eq. (2) with the canonical HF orbital replaced by a momentum space Kohn–Sham orbital $\Psi_j^{KS}(\boldsymbol{p})$, and the electron correlation effect is accounted by the exchange-correlation potential.

EMS measurements in this work are undertaken with the symmetric non-coplanar geometry using a

* Supported by the National Natural Science Foundation of China under Grant No 10575062, and the Specialized Research Fund for the Doctoral Programme of Higher Education under Grant No 20050003084.

** To whom correspondence should be addressed. Email: djk-dmp@mail.tsinghua.edu.cn

newly developed high resolution and high sensitivity $(e, 2e)$ electron momentum spectrometer.[11] The binding energy spectra (BES) are collected simultaneously at a range of azimuthal angles $\phi = -38°$ to $+38°$. Electron density distributions are obtained by deconvolution of the same peak from the binding energy spectrum at different azimuthal angles. Relying on the significant improvement of coincidence count rate and the good resolution performance ($\Delta\theta = \pm 0.7°$, $\Delta\phi = \pm 1.9°$, and $\Delta E = \pm 1.2$ eV), the binding energy and electron momentum distributions can be obtained accurately within a proper experimental period.

Theoretical calculations of the momentum profiles are carried out using the GAUSSIAN98 programme, and the geometric parameters (HF/6-311G**) for the chair conformer are obtained from NIST Standard Reference Database.[12] The sample of 1,4-dioxane is 99.5% in purity, and is used without further purification.

The chair form of 1,4-dioxane has C_{2h} point group symmetry, according to the HF/6-311++G** orbital energy order, its electronic configuration can be written as $(1b_u)^2(1a_g)^2(1a_u)^2(2a_g)^2(1b_g)^2(2b_u)^2(3a_g)^2(3b_u)^2(2a_u)^2 \quad (4a_g)^2(2b_g)^2 4(4b_u)^2(5a_g)^2(3b_g)^2(5b_u)^2 \quad (6a_g)^2(3a_u)^2(6b_u)^2(4a_u)^2(5a_u)^2(4b_g)^2 \quad (7a_g)^2(7b_u)^2(8a_g)^2$. By using DFT-B3LYP/6-311++G** method, the electronic configuration is predicted to be $(1a_g)^2(1b_u)^2(1a_u)^2(2a_g)^2(1b_g)^2(2b_u)^2 \quad (3a_g)^2(3b_u)^2(2a_u)^2(4a_g)^2(2b_g)^2(4b_u)^2(5a_g)^2(3b_g)^2 \quad (3a_u)^2(5b_u)^2(6a_g)^2(4a_u)^2(6b_u)^2(5a_u)^2(4b_g)^2(7a_g)^2 \ (7b_u)^2(8a_g)^2$.

It can be seen that besides the reversal of first two orbitals ($1b_u$ and $1a_g$), the ordering of MO_{15} to MO_{19} is predicted discordantly by both the HF and DFT methods.

The binding energy spectra of 1,4-dioxane at impact energy of 600 eV is shown in Fig. 1. There are eight peaks that can be clearly identified, and the corresponding experimental binding energies are 9.4, 10.9, 13.1, 16.3, 19.3, 22.1, 24.6 and 32.1 eV, respectively. The EMS binding energy results of all valence orbitals are listed in Table 1 in comparison with the high resolution photoelectron spectroscopy (PES) results.[13,14] The ionization peaks for HOMO, MO_{12} and MO_9 (correspond to peaks 1, 5, and 7) are well resolved, while the other fifteen orbitals, due to their small energy intervals, are not well separated, thus peaks 2, 3, 4, 6, and 8 contain their combination of MO_{22} + MO_{23}, MO_{18} + MO_{19} + MO_{20} + MO_{21}, MO_{13} + MO_{14} + MO_{15} + MO_{16} + MO_{17}, MO_{10} + MO_{11} and MO_7 + MO_8 + satellites, respectively. The orbital ordering discord of MO_{15} to MO_{19} can be viewed more expressly in Table 1. The HF and DFT methods give opposite orderings for MO_{18} and MO_{19}, and the orderings of MO_{15} MO_{16} and MO_{17} are predicted to be $3a_u < 6a_g < 5b_u$ and $6b_g < 5b_u < 3a_u$, respectively. However, according to the orbital distribution, the ordering differences can not be distinguished experimentally as the corresponding orbitals are contained in same peaks.

Table 1. PES and EMS binding energies of valence orbitals of 1,4-dioxane.

Orbital			Binding energy (eV)		
MO	RHF	DFT	PES[13]	PES[14]	EMS
24	$8a_g$	$8a_g$	9.43	9.4	9.4
23	$7b_u$	$7b_u$	10.73	10.6	10.9
22	$7a_g$	$7a_g$	11.27	11.2	
21	$4b_g$	$4b_g$	12.9	12.5∼13.7	13.1
20	$5a_u$	$5a_u$	13.2		
19	$4a_u$	$6b_u$			
18	$6b_u$	$4a_u$	14.1	14.0	
17	$3a_u$	$6a_g$	15.1	15.4	
16	$6a_g$	$5b_u$			
15	$5b_u$	$3a_u$	16.2	15.7∼16.7	16.3
14	$3b_g$	$3b_g$			
13	$5a_g$	$5a_g$	17.2	17.1	
12	$4b_u$	$4b_u$	19.4	19.3	19.3
11	$2b_g$	$2b_g$		21.5	22.1
10	$4a_g$	$4a_g$		22.5	
9	$2a_u$	$2a_u$		24.7	24.6
8	$3b_u$	$3b_u$			32.1
7	$3a_g$	$3a_g$			

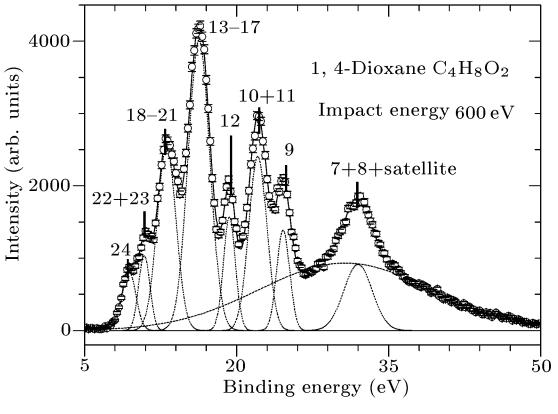

Fig. 1. Binding energy spectra of 1, 4-dioxane with 600 eV impact energy. The dotted lines represent individual Gaussian fits and the solid line represents the summed fit.

Figure 2 shows the experimental and theoretical momentum profiles of HOMO. Theoretical calculations are carried out by using the HF and DFT-B3LYP methods with 6-311++G** and AUG-CC-PVTZ basis sets. The theoretical momentum profiles can be regarded as mixed "s–p-type" profile, which exhibits two maxima of electron density at $p = 0$ and 1.35 a.u. HF and DFT calculations give different relative intensities in the low momentum region and profiles of the DFT-B3LYP method (curves 2 and 4) are in agreement well with the experimental results. In the momentum range above 1.0 a.u., the experimental profile can not be well described by any of the four theoretical profiles, the discrepancy might be caused by the lower

coincidence counting rate in the larger azimuthal angle (correspond to the higher momentum) area and accordingly the bigger uncertainty in the deconvolution process.

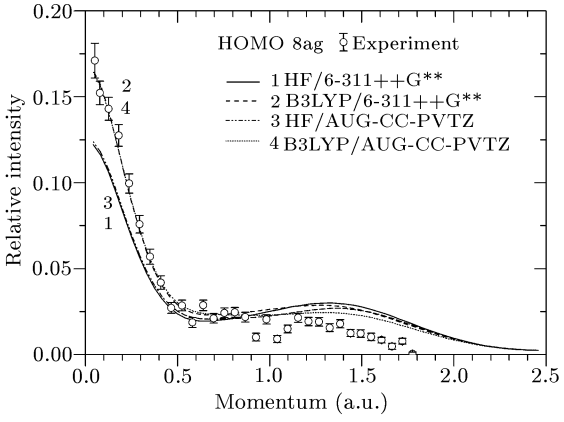

Fig. 2. Experimental and calculated momentum distribution for HOMO (MO_{24}: $8a_g$). Theoretical momentum profiles are calculated by using the HF and DFT methods with the 6-311++G** and AUG-CC-PVTZ basis sets.

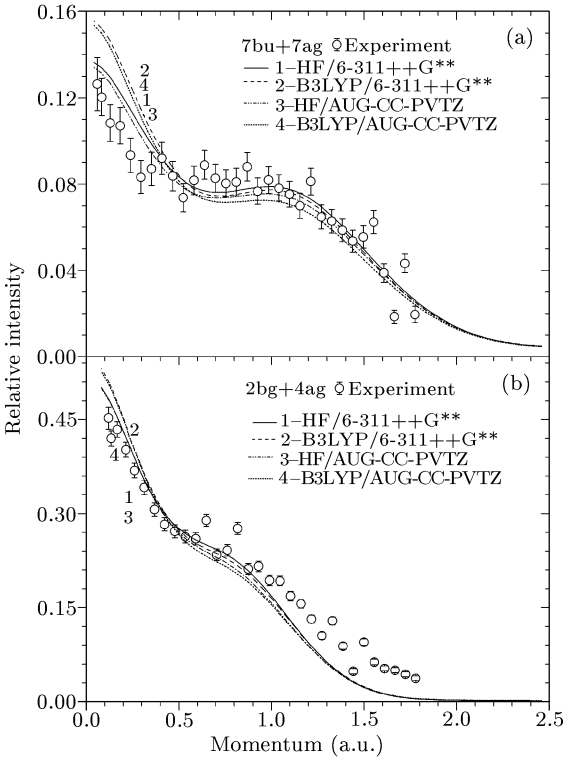

Fig. 3. Experimental and theoretical momentum distribution for (a) peak 2 (MO_{23} + MO_{22}: $7b_u + 7a_g$), (b) peak 6 (MO_{11} + MO_{10}: $2b_g + 4a_g$).

The momentum distributions of peak 2 ($7b_u + 7a_g$) and peak 6 ($2b_g + 4a_g$) have the similar profile type (see Fig. 3), such as the case in the HOMO theoretical profiles. The DFT method (curve 2 and 4) predicts higher electron density in the low momentum region than the HF method (curves 1 and 3), whereas it is in contrast with the case of the HOMO that the experimental results are closer to the HF theoretical profiles, but it is still not very convincing to say that the HF method shows better performance than the DFT method since the experimental results in low momentum region of ($7b_u + 7a_g$) have relatively large uncertainty and theoretical profiles of ($2b_g + 4a_g$) are not well distinguished. It can be seen from Fig. 3(b) that the experimental profile turns up in momentum region above 1.0 a.u., which can not be well described by any of the theoretical calculations.

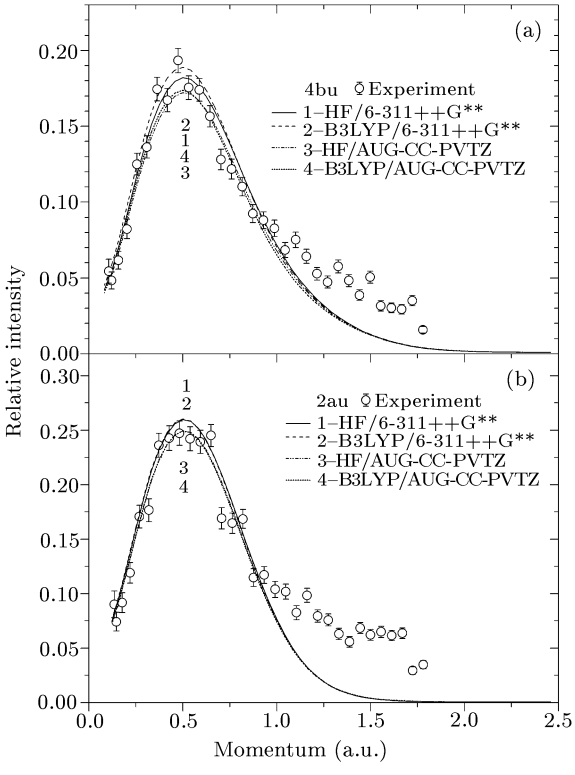

Fig. 4. Experimental and theoretical momentum distribution for (a) peak 5 (MO_{12}: $4b_u$), (b) peak 7 (MO_9: $2a_u$).

As is shown in Fig. 4, MO_{12} ($4b_u$) and MO_9 ($2a_u$) both have the '*p*-type' profile which exhibits a maximum of electron density at $p = 0.5$ a.u. The peak values of relative intensity are differently predicted by various calculations in Fig. 4(a), while in Fig. 4(b), curves 1 and 2 as well as curves 3 and 4 are not distinguishable, respectively, and the theoretical profiles of both the HF and DFT method with AUG-CC-PVTZ basis set (curves 3 and 4) are in slightly better agreement with the experimental results than the 6-311++G** basis set. In the high momentum region above 1.0 a.u., the 'turn-up' of the experimental profile observed in ($2b_g + 4a_g$) can also be found in $4b_u$ and $2a_u$ orbitals. A possible explanation for the discrepancies is the distorted wave effect since the plane wave

impulse approximation is invalid at higher momentum region.[9,15−18]

In summary, the binding energy spectrum of all valence orbitals and the momentum distributions of HOMO and other four sets of valence orbitals in 1,4-dioxane have been investigated by electron momentum spectroscopy. The experimental results are compared with theoretical calculations of C_{2h} conformation using the HF and DFT methods with the 6-311++G** and AUG-CC-PVTZ basis sets. The experimental profiles of the investigated orbitals are consistent with theoretical calculations, and it appears that the DFT method achieves relatively better descriptions for the momentum distributions. The AUG-CC-PVTZ basis set shows the performance slightly better than the 6-311++G** basis set. These results also confirm the prediction of C_{2h} conformation for 1,4-dioxane made in other studies.

References

[1] Bako I, Palinkas G, Dore J and Fischer H 1999 *Mol. Phys.* **96** 743

[2] Mohr T 2001 *Solvent Stabilizers White Paper* (Santa Clara Valley Water District)

[3] Satila S K, Wang C H 1977 *Chem. Phys. Lett.* **46** 1892

[4] Estaban A L, Galanche M 1994 *Mol. Phys.* **82** 303

[5] Takamuku T, Nakamizo A, Tabata M et al 2003 *J. Mol. Liq.* **103-104** 143

[6] Chapman D, Hester R E 1997 *J. Phys. Chem.* A **101** 3382

[7] McCarthy I E, Weigold E 1991 *Rep. Prog. Phys.* **54** 789

[8] Coplan M A, Moore J H, Doering J P 1994 *Rev. Mod. Phys.* **66** 985

[9] Weigold E, McCarthy I E 1999 *Electron Momentum Spectroscopy* (New York: Kulwer)

[10] Duffy P, Chong D P, Casida M E and Salahub D R 1994 *Phys. Rev.* A **50** 4707

[11] Ren X G, Ning C G, Deng J K et al 2005 *Rev. Sci. Instrum.* **76** 063103

[12] http://srdata.nist.gov/cccbdb/

[13] Kimura K, Katsuwata S, Achiba Y, Yamazaki T, Iwata S 1981 *Handbook of HeI Photoelectron Spectra of Fundamental Organic Molecules* (New York: Halsted Press)

[14] Bieri G, Asbrink L, von Niessen W 1982 *J. Electron Spectrosc. Relat. Phenom.* **27** 129

[15] Deng J K, Li G Q, Huang J D et al 2002 *Chin. Phys. Lett.* **19** 47

[16] Xu C K, Chen X J, Jia C C et al 2002 *Chin. Phys. Lett.* **19** 1795

[17] Ren X G, Ning C G et al 2005 *Chem. Phys. Lett.* **404** 279

[18] Zhang S F, Ning C G et al 2006 *Chin. Phys. Lett.* **23** 583